Atmos. Chem. Phys. Discuss., 15, 14403–14443, 2015
www.atmos-chem-phys-discuss.net/15/14403/2015/
doi:10.5194/acpd-15-14403-2015

Atmospheric Chemistry and Physics Discussions

Organic aerosol evolution and transport observed at Mt. Cimone (2165 m a.s.l.), Italy, during the PEGASOS campaign

M. Rinaldi[1], S. Gilardoni[1], M. Paglione[1], S. Decesari[1], S. Sandrini[1], S. Fuzzi[1], P. Massoli[2], P. Bonasoni[1], P. Cristofanelli[1], A. Marinoni[1], V. Poluzzi[3], and M. C. Facchini[1]

[1]National Research Council, Institute of Atmospheric Sciences and Climate, Bologna, Italy
[2]Aerodyne Research Inc., Billerica, MA, USA
[3]Centro Tematico Regionale Aree Urbane, Arpa Emilia-Romagna, Bologna, Italy

Received: 30 March 2015 – Accepted: 29 April 2015 – Published: 22 May 2015

Correspondence to: M. Rinaldi (m.rinaldi@isac.cnr.it)

Published by Copernicus Publications on behalf of the European Geosciences Union.

Abstract

High resolution aerosol mass spectrometer measurements have been performed, for the first time, at the Mt. Cimone Global Atmospheric Watch (GAW) station between June and July 2012, within the EU project PEGASOS and the ARPA–Emilia Romagna project SUPERSITO. Sub-micron aerosol was dominated by organics (63 %) with sulphate, ammonium and nitrate contributing for the remaining 20, 9 and 7 %, respectively. Organic aerosol (OA) was in general highly oxygenated, consistent with the remote character of the site; our observations suggest that oxidation and secondary organic aerosol (SOA) formation processes occurred during aerosol transport to high altitudes. All of the aerosol component concentrations as well as the OA elemental ratios showed a clear daily trend, driven by the evolution of the planetary boundary layer (PBL) and by the mountain wind regime. Higher loadings and lower OA oxidation levels were observed during the day, when the site was within the PBL, and therefore affected by relatively fresh aerosol transported from lower altitudes. Conversely, lower loadings and higher OA oxidation levels were observed at night, when the top of Mt. Cimone resided in the free troposphere although affected by the transport of residual layers on several days of the campaign. Analysis of the elemental ratios in a Van Krevelen space shows that OA oxidation follows a slope comprised between −0.5 and −1, consistent with addition of carboxylic groups, with or without fragmentation of the parent molecules. The increase of carboxylic groups during OA ageing is confirmed by the increased contribution of organic fragments containing more than one oxygen atom in the free troposphere night-time mass spectra. Finally, positive matrix factorization was able to deconvolve the contributions of relatively fresh OA (OOAa) originating from the PBL, more aged OA (OOAb) present at high altitudes during periods of atmospheric stagnation, and very aged aerosols (OOAc) transported over long distances in the free troposphere.

ACPD
15, 14403–14443, 2015

1 Introduction

Atmospheric aerosols have been intensively studied in the last decades because of their effects on climate, air quality and ecosystems. In many environments, organic aerosol (OA) constitutes a dominant fraction of submicron particles mass (Zhang et al., 2007; Jimenez et al., 2009). OA is made of thousands of individual compounds that can either be emitted directly into the atmosphere (i.e., primary OA or POA) or formed through chemical and physical processes (i.e. secondary OA or SOA). Given the extremely wide range of properties (polarity, vapour pressure, etc.) and number of compounds, typically only 10–20 % of the OA mass can be speciated at the molecular level (Seinfeld and Pankow, 2003).

OA is a dynamic component, experiencing both atmospheric oxidation and reversible partitioning. This processing (usually referred as ageing) is generally not completely understood and not well represented in models (Heald et al., 2010). In the last decade, on-line instruments like the Aerodyne Research Inc. Aerosol Mass Spectrometer (AMS) (Jayne et al., 2000; Canagaratna et al., 2007) have provided new insights into OA chemical composition and simplified ways of characterizing atmospheric OA ageing. Ng et al. (2010) showed that OA composition tends to become less variable with photochemical ageing, regardless of their source, with the most oxidized spectra resembling that of fulvic acid. Heald et al. (2010) applied the Van Krevelen diagram (H : C vs. O : C space) to the elemental composition of ambient and laboratory OA, observing that bulk OA elemental ratios follow a line characterized by a slope of −1. This implies that OA ageing involves, on average, the addition of carboxylic acids or equal amounts of hydroxyl and carbonyl functionalities. By contrast, based on a worldwide dataset, Ng et al. (2011) observed a slope of ∼ −0.5 for the oxidation of SOA which is characteristic of addition of alcohol, carbonyl and carboxyl functionalities during the ageing process, or of the addition of carboxylic groups accompanied by a C-C bond cleavage (molecular fragmentation). Recently, Holzinger et al. (2013) showed that fragmentation gains importance over functionalization as photochemical age of OA in-

ACPD
15, 14403–14443, 2015

creases, as originally proposed by Kroll et al. (2009). Finally, both ambient observations (Jimenez et al., 2009; Morgan et al., 2010) and laboratory studies (Massoli et al., 2010; Lambe et al., 2011) have pointed out that atmospheric ageing lowers OA volatility and enhances their hygroscopicity, evidencing the importance of atmospheric processing in determining the OA climate relevant properties.

In this study, we investigate the atmospheric processing of OA over the Po Valley basin, taking advantage of the unique observatory of Mt. Cimone, part of the Global Atmospheric Watch (GAW) network, by World Meteorological Organization (WMO), a suitable location to study tropospheric background conditions. Moreover, mountain sites close to anthropogenically-impacted areas provide the opportunity to investigate transport and chemical processing of polluted air masses lifted by convection or by pressure gradients on the mountain slopes (valley breezes) (Marinoni et al., 2008; Gilardoni et al., 2009).

The first AMS measurements performed at high altitude mountain stations were reported by Hock et al. (2008) and by Lanz et al. (2008). In particular, the latter study highlighted lower concentrations and higher oxygen content in aerosols collected at the Hohenpeissenberg (Germany) and Jungfraujoch (Switzerland) stations compared to measurement performed simultaneously at low altitude sites. Sun et al. (2009) and Freney et al. (2011) confirmed these findings with measurements performed at Whistler Mountain (Canada), and Puy-de-Dome (France), respectively, and provided useful insights of seasonal effects and air mass origin on the physico-chemical properties of regional aerosol particles measured at elevated sites.

The Mt. Cimone GAW/WMO Station is a high altitude research site located in the north Italian Apennines, facing the heavily populated and industrialized Po Valley region. In this study, we present and discuss online sub-micron aerosol chemical composition data collected at Mt. Cimone by high resolution time of flight aerosol mass spectrometer, HR-ToF-AMS (DeCarlo et al., 2006), during summer 2012, within the EU project PEGASOS and of the Agenzia Regionale per la Prevenzione e l'Ambiente (ARPA) – Emilia Romagna SUPERSITO project. The measurements were used to

ACPD
15, 14403–14443, 2015

characterize the summer background aerosol transported into the Po Valley basin area, the vertical transport of anthropogenic aerosol from the lower troposphere (typical of summer circulation), and the regional scale oxidation of OA. Prior to this study, aerosol chemical composition data for Mt. Cimone station were reported by Putaud et al. (2004), Marenco et al. (2006) and Carbone et al. (2010, 2014) using offline aerosol characterization techniques (i.e., filter samples analysed by ion chromatography and organic carbon analysis). All these papers evidenced the importance of the OA fraction in sub-micron aerosol at the site, both in summer and winter conditions. However, this is the first time that online characterization of atmospheric aerosol at high resolution, and particularly of OA, is reported for a high mountain site in Italy, at the centre of the Mediterranean climate hot-spot region.

2 Methods

2.1 Sampling site

Mt. Cimone is the highest peak of the North Italian Apennines. The top of Mt. Cimone (44°11′ N, 10°42′ E, 2165 m a.s.l.) hosts the Italian Climate Observatory "O. Vittori" that is part of the GAW program of the WMO. The station is situated at the southern border of the Po Valley, which is a highly populated and industrialized area, also characterized by intense agricultural activities. Anticyclonic conditions often favour a reduced ventilation within the basin promoting the build-up of lower troposphere aerosols and pollutants.

Measurements of atmospheric components carried out at this site are generally considered representative for the South European free troposphere (Bonasoni et al., 2000; Fischer et al., 2003). Nevertheless, due to enhanced vertical mixing occurring during summer months, a daytime influence at Mt. Cimone from the PBL has been documented (Fischer et al., 2003; Cristofanelli et al., 2007). For these reasons, this measurement site can represent a suitable location to investigate the influence of both local

ACPD
15, 14403–14443, 2015

and long range transport of polluted air masses on the free troposphere composition (Marinoni et al., 2008).

2.2 Online aerosol chemical characterization

The mass loading and the size-resolved chemical composition of submicron aerosol particles was characterized online by a HR-ToF-AMS. The HR-ToF-AMS provides measurements of the non-refractory sulfate, nitrate, ammonium, chloride, and organic mass in submicron particles (NR-PM_1). During the whole campaign, the HR-ToF-AMS was operating by alternating between "V" and "W" ion path modes every 5 min. The V mode is characterized by higher sensitivity and lower mass resolution, while the W mode provides higher mass resolution, but lower sensitivity. The concentrations reported here correspond to the data collected in V mode. In V mode, the instrument also acquires information about size distribution of particles, or particle time-of-flight, pToF (Jimenez et al., 2003). The AMS has an effective 50 % cut-off for particle sizes below 80 nm and above 600 nm in vacuum aerodynamic diameter (d_{va}) as determined by the transmission characteristics of the standard aerodynamic lens (Liu et al., 2007). Changes in ambient pressure may lead to changes in particle velocity in the AMS and lens transmission efficiencies (Liu et al., 2007; Bahreini et al., 2008). However, such effects are not expected to be significant at the pressure conditions typical of Mt. Cimone (Liu et al., 2007; Sun et al., 2009).

All data were analysed using standard ToF-AMS Analysis software SQUIRREL v1.51 and PIKA v1.10 (D. Sueper, available at: http://cires.colorado.edu/jimenez-group/ToFAMSResources/ToFSoftware/index.html) within Igor Pro 6.2.1 (WaveMetrics, Lake Oswego, OR). Positive matrix factorization (PMF) analyses on the HR-ToF-AMS data were performed using the PMF2.exe algorithm (v.4.2) in robust mode (Paatero and Tapper, 1994). The PMF inputs (mass spectral and error matrices of the OA component) were prepared according to Zhang et al. (2011). The PMF solutions were then evaluated with an Igor Pro-based PMF evaluation tool (PET, v. 2.04) following the method described in Ulbrich et al. (2009) and Zhang et al. (2011). The HR-ToF-AMS collection

ACPD
15, 14403–14443, 2015

efficiency (CE) was calculated according to Middlebrook et al. (2012) and evaluated against parallel offline measurements (Fig. S1). The average CE for the campaign was 0.52 ± 0.06.

2.3 Additional measurements

Ancillary measurements at Mt. Cimone conducted during the campaign include meteorological parameters, aerosols and trace gases (CO, O_3, NO_x). Trace gas measurements were carried out by using a common sampling system expressly designed for reactive gas sampling. Surface ozone (O_3) was continuously measured (1 min time resolution) by a UV-absorbtion analyser Dasibi 1108 W/GEN (see more details by Cristofanelli et al., 2015). Carbon dioxide (CO) was measured by a NDIR analyser Thermo Tei 49C. Following Henne et al. (2008), the system and sampling procedures have been modified to carry out observations in remote conditions usually characterized by low mixing ratios. During the PEGASOS 2012 campaign, NO_x measurements were carried out by a chemioluminescence analyser (Thermo 42C). This instrument is equipped with molybdenum converter for determination of NO_x thus, according to Steinbacher et al. (2007), the NO_2 reading can be overestimated up to $\sim 50\,\%$ due to the interference of other oxidized nitrogen compounds (NO_y) such as peroxyacetylnitrate and nitric acid.

The measurement of the aerosol absorption coefficient was obtained by a Multi-Angle Absorption Photometer (MAAP 5012, Thermo Electron Corporation), that measures the transmission and the back scattering of a light beam incident on a fiber filter where aerosol particles are deposited by sampling flow. The equivalent black carbon (eqBC) concentration has been obtained by using a mass absorption efficiency of $6.5\,m^2\,g^{-1}$ as recommended by Petzold et al. (2002) and set by default on MAAP.

PM_1 offline aerosol samples were collected on quartz filters as described by Carbone et al. (2014) with a 12 h sampling resolution. Chemical analysis of main inorganic species was performed via ion chromatography and carbon elemental analysis (Carbone et al., 2014).

ACPD
15, 14403–14443, 2015

3 Results

3.1 Online aerosol chemical characterization at Mt. Cimone

Figure 1 shows the time trend of the major non-refractory components of submicron aerosol (NR-PM_1) measured at Mt. Cimone during the campaign, together with the time dependent relative mass contribution of the same aerosol components. NR-PM_1 was clearly dominated by OA through the whole campaign: OA average atmospheric concentration was $2.8 \pm 2.4\,\mu g\,m^{-3}$ for an average mass contribution of 63 %. Sulphate was the second contributor with an average concentration of $0.92 \pm 0.60\,\mu g\,m^{-3}$ (20 %), followed by ammonium ($0.41 \pm 0.33\,\mu g\,m^{-3}$, 9 %) and nitrate ($0.33 \pm 0.46\,\mu g\,m^{-3}$, 7 %). Chlorine was usually below the detection limit (80 % of the data points) and contributed less than 1 % to the NR-PM_1 (and was therefore excluded from Fig. 1b). For comparison, aerosol chemical characterization measurements performed in spring and summer at high (Jungfraujoch) and rural (Hohenpeissenberg) sites in Europe (Hock et al., 2008; Lanz et al., 2010) report organics ranging from 43 to 50 %, sulphate ranging from 19 to 26 %, ammonium contributing between 13 and 11 % and nitrate ranging from 18 to 19 % (see Table 1 for a summary of AMS measurements performed at background measurements sites).

The measured ammonium concentrations were in equivalent concentrations to the sum of sulphate, nitrate and chloride, with a slope of 0.99 and a linear correlation coefficient (R) of 0.99. This means that aerosol particles measured at Mt. Cimone have no free acidity. The average NR-PM_1 mass during the campaign was $4.5 \pm 3.4\,\mu g\,m^{-3}$, in fairly good agreement with PM_1 measurements previously performed at the site in the same season, even though with different measurement techniques (Marenco et al., 2006; Carbone et al., 2010, 2014). The lowest aerosol mass concentrations were observed during the first days of the campaign up to 15 June, when Northern Italy was influenced by a low-pressure system, bringing unstable conditions. Conversely, the highest concentrations were recorded between 17 and 20 June under high pressure conditions characterized by anti-cyclonic circulation (Decesari et al., 2015), which is

ACPD
15, 14403–14443, 2015

known to favour the stagnation of local pollutants produced within the Po Valley basin (see Fig. S2 for further details).

The results of the elemental analysis (EA) of the organic fraction are presented in Fig. 2 as time trends of the H : C, O : C and OM : OC ratios. Average H : C, O : C and OM : OC ratio measured during the campaign are 1.45 ± 0.11, 0.71 ± 0.08 and 2.08 ± 0.10, respectively, corresponding to an average oxidation state ($OS_C = 2 \times O:C - H:C$; Kroll et al., 2011) of -0.02 ± 0.23. These ratios are indicative of a highly oxygenated organic aerosol, in agreement with previous AMS measurements at mountain sites (Freney et al., 2011; Lanz et al., 2010). The values have been calculated using the improved-Ambient (I-A) EA method to derive OA elemental ratios from AMS spectra (Canagaratna et al., 2015).

The corresponding EA values calculated using the Aiken-Ambient (A-A) method (Aiken et al., 2008), are 1.32 ± 0.08, 0.58 ± 0.07 and 1.89 ± 0.09, respectively, corresponding to an average oxidation state ($OS_C = 2 \times O:C - H:C$) of -0.16 ± 0.22. The elemental ratios calculated with the A-A method are reported here just for the purpose of a more direct comparison with previous works. Anyway, through all the paper and in the plots, the more accurate I-A elemental ratios will be reported. These ratios are similar to those presented by Mensah et al. (2012) for the rural background site of Cabauw (the Netherlands) during May 2008. Saarikoski et al. (2012) presents results of HR-ToF-AMS measurements in the Po Valley at the site of San Pietro Capofiume (SPC) during April 2008, showing an average H : C ratio slightly higher (1.49) and an average O : C ratio slightly lower (0.47) than those observed at Mt. Cimone, for a resulting average OM : OC ratio of 1.77. Similarly, OM : OC higher than 1.7 were observed in the outflow plume over Mexico city and at the mountain site of Altzomoni, above the Mexico city plateau (Gilardoni et al., 2009). The OM : OC ratio observed at SPC in Fall 2011 was 1.6 (Gilardoni et al., 2014). The lower oxidation of the OA collected at SPC during spring and fall with respect to the present measurements can be due to (a) the different season, being the atmosphere characterized by higher oxidative potential in full summer than in spring and fall, or (b) to oxidation processes involving OA during

ACPD
15, 14403–14443, 2015

transport from low altitude sites up to Mt. Cimone. This last aspect will be investigated in Sect. 3.3.

3.2 Analysis of the diurnal cycles

The atmospheric concentrations of the major NR-PM_1 components present a clear diurnal cycle with maxima at the early afternoon and minima during the night (Fig. 3). The concentration daily trend of the NR-PM_1 components is the result of the PBL dynamics and valley breezes, as during the night the site is well above the shallow nocturnal layer forming over the Po Valley plain and disconnected from the aerosol sources located at the low altitudes. However, Marinoni et al. (2008) showed that, in summer, during the night-time, Mt. Cimone station may be affected by polluted air masses present in the residual layer above the Po Valley. Conversely, during the day, with the increase of the PBL height, the site is affected by convective transport from lower altitudes (Schuepbach et al., 2001; Fischer et al., 2003; Freney et al., 2011) and it is directly connected to the pollution sources located in the valley, thus experiencing high aerosol concentrations. During PEGASOS, the time trend of OA (the major contributor to NR-PM_1) correlates with that of specific humidity (SH), which can be used as a tracer of PBL air at high altitudes (Henne et al., 2005) (Fig. S3). This good correlation strongly supports the hypothesis that the aerosol transport triggered by the PBL dynamics is the main factor regulating the NR-PM_1 concentrations at Mt. Cimone during the measurement period.

To further investigate the importance of vertical transport from the PBL to the top of Mt. Cimone during the day, we calculated the daily relative increase (RI) in SH, following the approach introduced by Prevôt et al. (2000) and Henne et al. (2005) for two different sites in the Alps and already applied for Mt. Cimone station by Carbone et al. (2014).

$$\mathrm{RI} = \frac{\mathrm{SH_{aft}\,(CMN)} - \mathrm{SH_{mor}\,(CMN)}}{\mathrm{SH_{aft}\,(SPC)} - \mathrm{SH_{mor}\,(CMN)}} \quad (1)$$

ACPD
15, 14403–14443, 2015

In Eq. (1), SH_{atf} (CMN) is the average specific humidity measured in the afternoon at Mt. Cimone (12:00 to 18:00 local time, LT), SH_{mor} (CMN) is the average specific humidity measured during the night at Mt. Cimone (22:00 to 05:00 LT) and SH_{aft} (SPC) is the average specific humidity measured in the afternoon (12:00 to 18:00 LT) at the rural background station of San Pietro Capofiume (SPC), located in the Po Valley 90 km north-east of Mt. Cimone at 11 m a.s.l. and considered representative of PBL conditions within the Po Valley basin. A RI of 1 corresponds to a complete replacement of the high altitude air by boundary layer air, while no vertical motion yields zero relative increase. RI was calculated for each day of the campaign and the average value resulted 0.8 ± 0.3, confirming the high influence of vertical convection during the day at the station in summer.

Similarly to the NR-PM_1 components, OA elemental ratios exhibit strong diurnal variations (Fig. 4). The O : C and OM : OC ratios have lower values in the afternoon and maxima at night, with a minimum O : C hourly average of 0.67 ± 0.10 observed between 14:00 and 15:00 LT, and maximum of 0.75 ± 0.08 between 00:00 and 01:00 LT. An opposite trend is observed for the H : C ratio, with a maximum hourly average of 1.55 ± 0.10 between 14:00 and 15:00 LT, and a minimum of 1.38 ± 0.10 between 00:00 and 01:00 LT. The daily trend of the O : C and OM : OC ratio are almost coincident (correlation coefficient 0.999) confirming the results of Pang et al. (2006) showing that the OM : OC ratio is mainly regulated by the O : C ratio.

These trends highlight the different age of the aerosols measured at the sampling location in different moments of the day, as a consequence of the PBL dynamics. In fact, the O : C ratio of OA tends to increase and the H : C ratio decreases as a function of its atmospheric residence time, because of the oxidation of reduced species emitted by traffic and combustion and of SOA formation (Aiken et al., 2008; DeCarlo et al., 2008; Heald et al., 2010; Chhabra et al., 2011; Ng et al., 2011; Sun et al., 2011a, b). Particles sampled at Mt. Cimone during the day are representative of an early stage of aerosol atmospheric oxidation, resulting from SOA formed at lower altitudes in the Po Valley and transported upward by turbulence and by thermal winds, typically in few hours.

ACPD
15, 14403–14443, 2015

By contrast, at night the aerosol sampled at Mt. Cimone is more processed, as the atmospheric layers affecting the site at night contain aerosols with an age from several hours (residual layers) to days (from long-range transport). This is confirmed by the CO / NO_x ratio, often used in the literature as a tracer for air mass photochemical age (Morgan et al., 2010; Freney et al., 2011). CO / NO_x at Mt. Cimone is 159 ± 65 during the daytime and 287 ± 168 at night, which is a value representative of aged regional emissions. For these reasons, Mt. Cimone is an ideal site to investigate the ageing of organic aerosol over the Po Valley basin. Moreover, according to Marinoni et al. (2008), the footprint of aerosol particles found in the residual layers at night comprises a great part of central Europe, and this corresponds to the region where the full oxidation of organic aerosols that we observed at Mt. Cimone also took place.

3.3 Investigation of regional scale organic aerosol ageing

To investigate the oxidation of OA, data collected at Mt. Cimone during the campaign have been divided based on the position of the station relative to the PBL height, using SH as a tracer of the PBL evolution. Figure S4 shows the average daily evolution of the SH at Mt. Cimone during the campaign that mimics the PBL evolution during the day: the afternoon maximum indicates that the site is within the PBL, under the influence of moist air coming from lower altitudes, while the night minimum indicates that Mt. Cimone station is above the PBL. Following Fig. S4, HR-ToF-AMS measurements collected between 12:00 and 18:00 have been considered as PBL samples, those collected between 22:00 and 05:00 have been defined as free troposphere (FT) samples, while all the samples excluded from the previous two groups have been considered as transition samples (TR). As expected, PBL samples resulted less oxidized ($H:C = 1.54 \pm 0.06$, $O:C = 0.69 \pm 0.05$, $OM:C = 2.05 \pm 0.10$) than FT samples ($H:C = 1.41 \pm 0.09$, $O:C = 0.74 \pm 0.07$, $OM:OC = 2.12 \pm 0.10$), with TR samples characterized by intermediate values ($H:C = 1.45 \pm 0.09$, $O:C = 0.72 \pm 0.07$, $OM:OC = 2.08 \pm 0.09$), consistent with the average elemental ratios discussed in the Sect. 3.1.

ACPD
15, 14403–14443, 2015

Figure 5 shows the whole campaign data points in a Van Krevelen diagram (Van Krevelen, 1950), together with the average H : C and O : C ratios of PBL, TR and FT samples. The data are lumped within the region delimited by O : C between 0.5 and 1 and H : C between 1.1 and 1.5. The plot illustrates synthetically the process of OA atmospheric oxidation in the investigated area, characterized by a slope comprised between −0.5 and −1. According to Heald et al. (2010) and Ng et al. (2011), such an intermediate slope can result from a combination of reactions adding carboxylic acids to the OA, occurring both with and without fragmentation of the parent molecules (expected slopes = −0.5 and −1, respectively). Kroll et al. (2011) reported that fragmentation becomes increasingly important for already oxidized material. This can explain the deviation from the −1 slope for Mt. Cimone, where direct sources of low oxidized OA are missing, in analogy with Ng et al. (2011). An alternative explanation for a slope tending to −0.5 is given by equivalent amounts of addition of carboxylic groups and of hydroxyls or peroxides (Ng et al., 2011).

The addition of carboxylic functionalities during the OA ageing process is confirmed by the analysis of the high resolution mass fragments, showing that, from PBL to FT samples, the average contribution of $C_xH_yO_{z>1}$, attributed to the fragmentation of carboxylic structures (Aiken et al., 2007; Takegawa et al., 2007; Duplissy et al., 2011), increases from 35 to 43 %, while both C_xH_y and C_xH_yO fragments decrease (Fig. 6). The mean elemental compositions calculated for PBL, TR and FT samples fall at distinct positions along the line of average ageing in the Van Krevelen space (Fig. 5), confirming that the observed oxidation of OA is dictated by the different age of the aerosols reaching the station at different times of the day.

Further information can be derived investigating the particle size distribution observed during the three regimes (PBL, TR and RL). The average mass size distributions of the main NR-PM_1 components as measured by the HR-ToF-AMS are presented for PBL, TR and FT samples in Fig. 7. The Figure shows no appreciable size distribution difference between the three sample sub-sets, indicating no aerosol growth with ageing. This suggests that the observed increase of OA oxidation level is not due to the

ACPD
15, 14403–14443, 2015

condensation of highly oxidized vapours onto the particles, but to actual oxidation of particulate phase OA. Also, the fact that all the various NR-PM_1 species peak at the same average d_{va} of 300–350 nm suggests that they are rather well internally mixed.

3.4 OA source apportionment by PMF

In order to fully characterize the OA collected at Mt. Cimone, PMF was applied to the high-resolution OA mass spectra. We screened various solutions with a number of factors from two to ten. A 4-factor solution with rotational forcing parameter fPeak = 0 (Q/Q_{exp} = 2.3) was chosen, yielding four different types of OOA, two of which were recombined into one factor, because of coincident time series and profiles (Fig. S6). The OA components from the PMF analysis were identified by their mass spectra, elemental composition (Fig. 8) and diurnal cycles (Fig. 9), as well as by correlations of their time series with tracers (Table 2). A detailed summary of key diagnostic plots of the PMF results and a discussion of the factor solution choices can be found in the Supplement.

The three resulting factors are all of the oxygenated organic aerosol (OOA) type and have been defined as OOAa, OOAb and OOAc. No "standard" HOA factor (i.e., with m/z 43 $\gg$ m/z 44 and with a significant amount of hydrocarbon-like ions, C_xH_y) could be extracted by PMF, similarly to other AMS datasets collected at background sites (Hildebrandt et al., 2010; Freney et al., 2011), indicating a very low direct influence of (unprocessed) primary combustion aerosols to the observed OA load. This result is consistent with the highly oxidized character of the OA described previously. Even though m/z 44 (CO_2^+) dominates the mass spectra of all the three factors, the OOAa factor has a slightly higher amount of C_xH_y ions at m/z 27 ($C_2H_3^+$), 39 ($C_3H_3^+$), 41 ($C_3H_5^+$) compared to the other factors, which is consistent with its origin, discussed below.

The elemental composition (H : C, O : C) and the OM : OC ratio are also reported in Fig. 8. OOAc is the most oxidized factor, with an OM/OC ratio of 2.48 vs. 2.03 and 2.13 of OOAa and OOAb, respectively. Consequently, it has higher O : C (1.02)

ACPD
15, 14403–14443, 2015

and lower H : C (1.07) ratio than OOAa (0.67; 1.51) and OOAb (0.75; 1.44). OOAa average concentration was $1.5 \pm 1.7\,\mu g\,m^{-3}$ during the campaign, which accounts for 55 % of the OA. OOAb presented higher concentrations during the period 17–23 June ($2.1 \pm 1.5\,\mu g\,m^{-3}$) and low concentrations during the rest of the campaign ($0.27 \pm 0.29\,\mu g\,m^{-3}$), for an average concentration of $0.67 \pm 1.1\,\mu g\,m^{-3}$ and a contribution of 25 %. The concentration of OOAc was $0.54 \pm 0.40\,\mu g\,m^{-3}$ contributing averagely 20 % to the OA.

When looking at the diurnal profiles of the three factors (Fig. 9), we see clear diurnal cycles for OOAa and OOAc (but with opposite trends, having OOAa a maximum at 16:00, and OOAc having a minimum at 14:00) and a less pronounced diurnal profile for OOAb (slightly higher concentration around 12:00–14:00 than during the rest of the day). The fact that OOAa concentration is much higher during the day than at night indicates that this factor derives from sources located within the PBL and is transported at Mt. Cimone by convection and by thermal winds in daytime, as discussed above. Conversely, the trend for OOAc with lower concentrations during the day points to a transport from the free troposphere, or anyway from above the PBL.

The Pearson correlation coefficients (R) between the three PMF factors and several external gas-phase and particle tracers are reported in Table 2. OOAa correlates best with CO, NO_x and BC (0.71, 0.70 and 0.54 respectively), which are attributable to anthropogenic sources located within the PBL, confirming our interpretation of the OOAa source location. OOAb shows lower correlation than OOAa against all the tracers, with higher R values associated with the above enlisted PBL tracers (CO, NO_x and BC), suggesting that this factor too was contributed by PBL sources. Interestingly, OOAb presents the highest correlation with sulphate, which suggests a regional character for this OOA component. The highest correlation for OOAc is with O_3, with a very small correlation with all the PBL tracers. The high correlation of OOAc with O_3 is mainly driven by the coincident daily trends (Fig. S7), showing higher concentration at night, a typical feature of O_3 at high-altitude sites (Fischer et al., 2003; Cristofanelli et al., 2007). In fact, during summer, air-masses richer in photochemically produced O_3 are

ACPD
15, 14403–14443, 2015

vented to Mt. Cimone in the afternoon, leading to an increase of O_3 along the afternoon until evening, when O_3 observations started to be more representative of the free troposphere.

The spectral and elemental features of the three OOA factors are in the range of others reported in the literature (Mohr et al., 2012; Holzinger et al., 2013; Sun et al., 2011a). Similar OOA spectra have also been described by Saarikoski et al. (2012) for the Po Valley site of San Pietro Capofiume. Interestingly, the most oxidized OOA factor presented by Saarikoski et al. (2012) shares similar features with OOAc, with very high OM/OC ratios. Correlation analysis with reference high-resolution spectra (Table 3) suggests that all the OOA components identified can be classified as LV-OOA (low volatile-OOA), including the less oxygenated OOAa and OOAb. On the other hand, OOAa and OOAb present qualitatively similar spectral features to the SV-OOA (semi volatile-OOA) reported by Freney et al. (2011), for a similar high altitude station, and by Hayes et al. (2013), for photochemically aged aerosol. The f44 (contribution of organic mass fragments with m/z 44) of OOAa and OOAb is 0.13 and 0.14, respectively, which is across the SV-OOA/LV-OOA border region proposed by Cubison et al. (2011). Therefore, we believe that OOAa and OOAb can be considered either as highly oxidized SV-OOA or LV-OOA with a low oxidation level.

In summary, OOAa is clearly attributed to sources or formation processes located within the PBL that reach the station when vertical transport (PBL convection and valley/upslope breeze) is maximized. OOAa is the less aged factor retrieved by PMF and it likely represents a moderately aged local OA. OOAb has a less clear daily trend (still with maximum during daytime) and a slightly higher O : C ratio than OOAa, suggesting a higher atmospheric age. The period of OOAb maximum contribution coincides with meteorological conditions characterized by reduced horizontal air motion and dominated by breeze regimes (17–23 June, when an anticyclonic high pressure system was over northern Italy). These conditions favour the accumulation of pollutants within the PBL and in the residual layers above, because of reduced air circulation. Coen et al. (2011) demonstrated that under such meteorological conditions, air masses from

ACPD
15, 14403–14443, 2015

residual layers continue to influence the Jungfraujoch high altitude station also during the night, leading to higher minima in the diurnal aerosol concentration than in other conditions. We postulate that the same happens at Mt. Cimone. The entire region influenced by the high pressure system extends beyond the Po Valley basin, comprising roughly the great Alpine region. Over the Alps, orographic lift of PBL air is responsible for the formation of residual layers at very high altitudes (the Jungfraujoch is at 3571 m a.s.l.) which can then travel on the top of the PBL over the surrounding basins (like the Po Valley), hence contributing to the "free tropospheric" conditions observed at Mt. Cimone. We hypothesize that factor OOAb is a regional component of NR-PM_1, associated with the accumulation and ageing of OA in residual layers when wind speeds are small throughout the lower troposphere during period of enhanced high pressure conditions. This is also supported by the good correlation between OOAb and sulphate.

Finally, OOAc is the product of prolonged atmospheric processing of OA, occurring mainly in the free troposphere, and can be considered as representative of the background FT OA on a spatial scale that comprises all western European areas upwind of Mt. Cimone. These conclusions are confirmed by the plots in Fig. 10, representing CO / NO_x vs. SH, colour coded by the contribution of each factor. Clearly, OOAa is associated with air masses characterized by reduced photochemical age (low CO / NO_x) and strongly influenced by the PBL (high SH), while OOAc contributes more in air masses characterized by high photochemical age (high CO / NO_x) and less influenced by the PBL (low SH). OOAb presents intermediate characteristics (mid to low CO / NO_x and intermediate SH), consistent with the hypothesis that OOAb is representative of OA of intermediate age that is accumulated in the residual layers during the period of high pressure, due to the stagnant atmospheric conditions.

4 Conclusions

The chemical composition of non-refractory sub-micrometric particles was measured for the first time by a HR-ToF-AMS at the Mt. Cimone high altitude station.

ACPD
15, 14403–14443, 2015

Sub-micrometric aerosol was dominated by the organic fraction (on average 63 %), with ammonium sulphate as second contributor, for an average NR-PM_1 mass of $4.5 \pm 3.4\,\mu g\,m^{-3}$. Elemental analysis of the high resolution AMS data showed highly oxygenated OA (the campaign-average H : C, O : C and OM : OC were 1.45 ± 0.11, 0.71 ± 0.08 and 2.08 ± 0.10, respectively), suggesting that strong oxidation and SOA formation processes occur during aerosol transport to high altitudes. Different stages of OA ageing could be characterized when comparing the composition during daytime, when the station was affected by the upward transport of PBL air, and at night-time when the site was in the free troposphere.

Analysis of the OA elemental ratios in a Van Krevelen space showed that OA oxidation followed a slope comprised between −0.5 and −1, consistent with the addition of carboxylic groups to alkyl structures, occurring both with and without fragmentation of the reagent molecules. The increase of carboxylic groups during OA ageing is confirmed by the increased contribution of $C_xH_yO_{z>1}$ fragments during night-time measurements (i.e., more aged). Analysis of the NR-PM_1 components size distribution shows no organic mass production during ageing, suggesting that heterogeneous reactions with gaseous oxidants were the dominant OA ageing process over the Po Valley basin during the investigated period.

Quantitative information on the contributions of more and less aged OA components were achieved by analysing the high resolution AMS data by positive matrix factorization (PMF). OOAa (55 %), the least oxidized OOA factor, was related to sources or formation processes located within the PBL, reaching the station mainly during day-time, when vertical transport is maximized. OOAb (25 %) was attributed to the accumulation and ageing of OA in the PBL and in the residual layers above the PBL, due to stagnation over the great Alpine region. Finally, OOAc (20 %) was interpreted as the product of prolonged atmospheric processing of OA, occurring mainly above the PBL, and can be considered as representative of background free tropospheric OA at a continental scale.

ACPD
15, 14403–14443, 2015

This work highlights the important contribution of organic aerosols to the composition of submicron particles at remote mountain sites. We found that 63 % of the NR-PM_1 mass that constitutes the background aerosol levels for the Po Valley in the summer, is accounted for by highly oxygenated organic matter. No important contribution from primary combustion organic particles (HOA) was measured, indicating that these compounds were likely lost during transport either by evaporation or chemical processing. Most importantly, in spite of the vicinity of strongly emitting pollution sources in the Po Valley, only 55 % of the organic matter measured at Mt. Cimone in the summer could be attributed to sources within the PBL, while the remaining fraction (45 %) is accounted for by remote upwind sources. This study confirms the importance of regional scale physical and chemical processes and of transboundary transport in determining the background aerosol composition at rural European sites.

The Supplement related to this article is available online at doi:10.5194/acpd-15-14403-2015-supplement.

Acknowledgements. This work was supported by the projects PEGASOS and BACCHUS funded by the European Commission under the Framework Programme 7 (FP7-ENV-2010-265148 and FP7-603445) and by the project SUPERSITO funded by Regione Emilia Romagna (DRG no. 428/10). Continuous atmospheric observation programmes at Mt. Cimone are supported by the Project of National Interest NextData, funded by Italian Ministry for Education, University and Research and by EU-ACTRIS project.

Leone Tarozzi, Francesca Pollini and Francescopiero Calzolari are acknowledged for the technical support.

ACPD
15, 14403–14443, 2015

References

Aiken, A. C., DeCarlo, P. F., and Jimenez, J. L.: Elemental analysis of organic species with electron ionization high-resolution mass spectrometry, Anal. Chem., 79, 8350–8358, doi:10.1021/ac071150w, 2007.

Aiken, A. C., Decarlo, P. F., Kroll, J. H., Worsnop, D. R., Huffman, J. A., Docherty, K. S., Ulbrich, I. M., Mohr, C., Kimmel, J. R., Sueper, D., Sun, Y., Zhang, Q., Trimborn, A., Northway, M., Ziemann, P. J., Canagaratna, M. R., Onasch, T. B., Alfarra, M. R., Prevot, A. S. H., Dommen, J., Duplissy, J., Metzger, A., Baltensperger, U., and Jimenez, J. L.: O/C and OM/OC ratios of primary, secondary, and ambient organic aerosols with high-resolution time-of-flight aerosol mass spectrometry, Environ. Sci. Technol., 42, 4478–4485, doi:10.1021/es703009q, 2008.

Bahreini, R., Dunlea, E. J., Matthew, B. M., Simons, C., Docherty, K. S., DeCarlo, P. F., Jimenez, J. L., Brock, C. A., and Middlebrook, A. M.: Design and operation of a pressure-controlled inlet for airborne sampling with an aerodynamic aerosol lens, Aerosol Sci. Tech., 42, 465–471, doi:10.1080/02786820802178514, 2008.

Bonasoni, P., Evangelisti, F., Bonafe, U., Ravegnani, F., Calzolari, F., Stohl, A., Tositti, L., Tubertini, O., and Colombo, T.: Stratospheric ozone intrusion episodes recorded at Mt. Cimone during the VOTALP project: case studies, Atmos. Environ., 34, 1355–1365, doi:10.1016/s1352-2310(99)00280-0, 2000.

Canagaratna, M., Jayne, J., Jimenez, J., Allan, J., Alfarra, M., Zhang, Q., Onasch, T., Drewnick, F., Coe, H., Middlebrook, A., Delia, A., Williams, L., Trimborn, A., Northway, M., DeCarlo, P., Kolb, C., Davidovits, P., and Worsnop, D.: Chemical and microphysical characterization of ambient aerosols with the aerodyne aerosol mass spectrometer, Mass Spectrom. Rev., 26, 185–222, doi:10.1002/mas.20115, 2007.

Canagaratna, M. R., Jimenez, J. L., Kroll, J. H., Chen, Q., Kessler, S. H., Massoli, P., Hildebrandt Ruiz, L., Fortner, E., Williams, L. R., Wilson, K. R., Surratt, J. D., Donahue, N. M., Jayne, J. T., and Worsnop, D. R.: Elemental ratio measurements of organic compounds using aerosol mass spectrometry: characterization, improved calibration, and implications, Atmos. Chem. Phys., 15, 253–272, doi:10.5194/acp-15-253-2015, 2015.

Carbone, C., Decesari, S., Mircea, M., Giulianelli, L., Finessi, E., Rinaldi, M., Fuzzi, S., Marinoni, A., Duchi, R., Perrino, C., Sargolini, T., Varde, M., Sprovieri, F., Gobbi, G. P., Angelini, F., and Facchini, M. C.: Size-resolved aerosol chemical composition over the Italian

ACPD
15, 14403–14443, 2015

Peninsula during typical summer and winter conditions, Atmos. Environ., 44, 5269–5278, doi:10.1016/j.atmosenv.2010.08.008, 2010.
Carbone, C., Decesari, S., Paglione, M., Giulianelli, L., Rinaldi, M., Marinoni, A., Cristofanelli, P., Didiodato, A., Bonasoni, P., Fuzzi, S., and Facchini, M. C.: 3-year chemical composition of free tropospheric PM_1 at the Mt. Cimone GAW global station – South Europe – 2165 m a.s.l., Atmos. Environ., 87, 218–227, doi:10.1016/j.atmosenv.2014.01.048, 2014.
Chhabra, P. S., Ng, N. L., Canagaratna, M. R., Corrigan, A. L., Russell, L. M., Worsnop, D. R., Flagan, R. C., and Seinfeld, J. H.: Elemental composition and oxidation of chamber organic aerosol, Atmos. Chem. Phys., 11, 8827–8845, doi:10.5194/acp-11-8827-2011, 2011.
Collaud Coen, M., Weingartner, E., Furger, M., Nyeki, S., Prévôt, A. S. H., Steinbacher, M., and Baltensperger, U.: Aerosol climatology and planetary boundary influence at the Jungfraujoch analyzed by synoptic weather types, Atmos. Chem. Phys., 11, 5931–5944, doi:10.5194/acp-11-5931-2011, 2011.
Cristofanelli, P., Bonasoni, P., Carboni, G., Calzolari, F., Casarola, L., Sajani, S. Z., and Santaguida, R.: Anomalous high ozone concentrations recorded at a high mountain station in Italy in summer 2003, Atmos. Environ., 41, 1383–1394, doi:10.1016/j.atmosenv.2006.10.017, 2007.
Cristofanelli, P., Scheel, H. E., Steinbacher, M., Saliba, M., Azzopardi, F., Ellul, R., Froehlich, M., Tositti, L., Brattich, E., Maione, M., Calzolari, F., Duchi, R., Landi, T. C., Marinoni, A., and Bonasoni, P.: Long-term surface ozone variability at Mt. Cimone WMO/GAW global station (2165 m a.s.l., Italy), Atmos. Environ., 101, 23–33, doi:10.1016/j.atmosenv.2014.11.012, 2015.
Cubison, M. J., Ortega, A. M., Hayes, P. L., Farmer, D. K., Day, D., Lechner, M. J., Brune, W. H., Apel, E., Diskin, G. S., Fisher, J. A., Fuelberg, H. E., Hecobian, A., Knapp, D. J., Mikoviny, T., Riemer, D., Sachse, G. W., Sessions, W., Weber, R. J., Weinheimer, A. J., Wisthaler, A., and Jimenez, J. L.: Effects of aging on organic aerosol from open biomass burning smoke in aircraft and laboratory studies, Atmos. Chem. Phys., 11, 12049–12064, doi:10.5194/acp-11-12049-2011, 2011.
DeCarlo, P., Kimmel, J., Trimborn, A., Northway, M., Jayne, J., Aiken, A., Gonin, M., Fuhrer, K., Horvath, T., Docherty, K., Worsnop, D., and Jimenez, J.: Field-deployable, high-resolution, time-of-flight aerosol mass spectrometer, Anal. Chem., 78, 8281–8289, doi:10.1021/ac061249n, 2006.

ACPD
15, 14403–14443, 2015

DeCarlo, P. F., Dunlea, E. J., Kimmel, J. R., Aiken, A. C., Sueper, D., Crounse, J., Wennberg, P. O., Emmons, L., Shinozuka, Y., Clarke, A., Zhou, J., Tomlinson, J., Collins, D. R., Knapp, D., Weinheimer, A. J., Montzka, D. D., Campos, T., and Jimenez, J. L.: Fast airborne aerosol size and chemistry measurements above Mexico City and Central Mexico during the MILAGRO campaign, Atmos. Chem. Phys., 8, 4027–4048, doi:10.5194/acp-8-4027-2008, 2008.

Decesari, S., Pandis, S., Mentel, T., Kindler-Schaar, A., Baltensperger, U., Wolf, R., Manninen, H., Sandrini, S., Gobbi, G. P., Fierli, F., Cristofanelli, P., Poluzzi, V., Bonafé, G., Morgillo, A., and Facchini M. C.: The 2012 PEGASOS-SUPERSITO Po Valley campaign: an overview, in preparation, 2015.

Duplissy, J., DeCarlo, P. F., Dommen, J., Alfarra, M. R., Metzger, A., Barmpadimos, I., Prevot, A. S. H., Weingartner, E., Tritscher, T., Gysel, M., Aiken, A. C., Jimenez, J. L., Canagaratna, M. R., Worsnop, D. R., Collins, D. R., Tomlinson, J., and Baltensperger, U.: Relating hygroscopicity and composition of organic aerosol particulate matter, Atmos. Chem. Phys., 11, 1155–1165, doi:10.5194/acp-11-1155-2011, 2011.

Fischer, H., Kormann, R., Klüpfel, T., Gurk, Ch., Königstedt, R., Parchatka, U., Mühle, J., Rhee, T. S., Brenninkmeijer, C. A. M., Bonasoni, P., and Stohl, A.: Ozone production and trace gas correlations during the June 2000 MINATROC intensive measurement campaign at Mt. Cimone, Atmos. Chem. Phys., 3, 725–738, doi:10.5194/acp-3-725-2003, 2003.

Freney, E. J., Sellegri, K., Canonaco, F., Boulon, J., Hervo, M., Weigel, R., Pichon, J. M., Colomb, A., Prévôt, A. S. H., and Laj, P.: Seasonal variations in aerosol particle composition at the puy-de-Dôme research station in France, Atmos. Chem. Phys., 11, 13047–13059, doi:10.5194/acp-11-13047-2011, 2011.

Gilardoni, S., Liu, S., Takahama, S., Russell, L. M., Allan, J. D., Steinbrecher, R., Jimenez, J. L., De Carlo, P. F., Dunlea, E. J., and Baumgardner, D.: Characterization of organic ambient aerosol during MIRAGE 2006 on three platforms, Atmos. Chem. Phys., 9, 5417–5432, doi:10.5194/acp-9-5417-2009, 2009.

Gilardoni, S., Massoli, P., Giulianelli, L., Rinaldi, M., Paglione, M., Pollini, F., Lanconelli, C., Poluzzi, V., Carbone, S., Hillamo, R., Russell, L. M., Facchini, M. C., and Fuzzi, S.: Fog scavenging of organic and inorganic aerosol in the Po Valley, Atmos. Chem. Phys., 14, 6967–6981, doi:10.5194/acp-14-6967-2014, 2014.

Hayes, P. L., Ortega, A. M., Cubison, M. J., Froyd, K. D., Zhao, Y., Cliff, S. S., Hu, W. W., Toohey, D. W., Flynn, J. H., Lefer, B. L., Grossberg, N., Alvarez, S., Rappenglueck, B., Tay-

ACPD
15, 14403–14443, 2015

lor, J. W., Allan, J. D., Holloway, J. S., Gilman, J. B., Kuster, W. C., De Gouw, J. A., Massoli, P., Zhang, X., Liu, J., Weber, R. J., Corrigan, A. L., Russell, L. M., Isaacman, G., Worton, D. R., Kreisberg, N. M., Goldstein, A. H., Thalman, R., Waxman, E. M., Volkamer, R., Lin, Y. H., Surratt, J. D., Kleindienst, T. E., Offenberg, J. H., Dusanter, S., Griffith, S., Stevens, P. S., Brioude, J., Angevine, W. M., and Jimenez, J. L.: Organic aerosol composition and sources in Pasadena, California, during the 2010 CalNex campaign, J. Geophys. Res.-Atmos., 118, 9233–9257, doi:10.1002/jgrd.50530, 2013.

Heald, C. L., Kroll, J. H., Jimenez, J. L., Docherty, K. S., DeCarlo, P. F., Aiken, A. C., Chen, Q., Martin, S. T., Farmer, D. K., and Artaxo, P.: A simplified description of the evolution of organic aerosol composition in the atmosphere, Geophys. Res. Lett., 37, L08803, doi:10.1029/2010gl042737, 2010.

Henne, S., Furger, M., and Prevot, A. S. H.: Climatology of mountain venting-induced elevated moisture layers in the lee of the Alps, J. Appl. Meteorol., 44, 620–633, doi:10.1175/jam2217.1, 2005.

Henne, S., Klausen, J., Junkermann, W., Kariuki, J. M., Aseyo, J. O., and Buchmann, B.: Representativeness and climatology of carbon monoxide and ozone at the global GAW station Mt. Kenya in equatorial Africa, Atmos. Chem. Phys., 8, 3119–3139, doi:10.5194/acp-8-3119-2008, 2008.

Hildebrandt, L., Kostenidou, E., Mihalopoulos, N., Worsnop, D., Donahue, N., and Pandis, S.: Formation of highly oxygenated organic aerosol in the atmosphere: insights from the Finokalia aerosol measurement experiments, Geophys. Res. Lett., 37, L23801, doi:10.1029/2010gl045193, 2010.

Hock, N., Schneider, J., Borrmann, S., Römpp, A., Moortgat, G., Franze, T., Schauer, C., Pöschl, U., Plass-Dülmer, C., and Berresheim, H.: Rural continental aerosol properties and processes observed during the Hohenpeissenberg Aerosol Characterization Experiment (HAZE2002), Atmos. Chem. Phys., 8, 603–623, doi:10.5194/acp-8-603-2008, 2008.

Holzinger, R., Goldstein, A. H., Hayes, P. L., Jimenez, J. L., and Timkovsky, J.: Chemical evolution of organic aerosol in Los Angeles during the CalNex 2010 study, Atmos. Chem. Phys., 13, 10125–10141, doi:10.5194/acp-13-10125-2013, 2013.

Jayne, J., Leard, D., Zhang, X., Davidovits, P., Smith, K., Kolb, C., and Worsnop, D.: Development of an aerosol mass spectrometer for size and composition analysis of submicron particles, Aerosol Sci. Tech., 33, 49–70, doi:10.1080/027868200410840, 2000.

ACPD
15, 14403–14443, 2015

Jimenez, J. L., Jayne, J. T., Shi, Q., Kolb, C. E., Worsnop, D. R., Yourshaw, I., Seinfeld, J. H., Flagan, R. C., Zhang, X. F., Smith, K. A., Morris, J. W., and Davidovits, P.: Ambient aerosol sampling using the Aerodyne aerosol mass spectrometer, J. Geophys. Res.-Atmos., 108, 8425, doi:10.1029/2001jd001213, 2003.

Jimenez, J., Canagaratna, M., Donahue, N., Prevot, A., Zhang, Q., Kroll, J., DeCarlo, P., Allan, J., Coe, H., Ng, N., Aiken, A., Docherty, K., Ulbrich, I., Grieshop, A., Robinson, A., Duplissy, J., Smith, J., Wilson, K., Lanz, V., Hueglin, C., Sun, Y., Tian, J., Laaksonen, A., Raatikainen, T., Rautiainen, J., Vaattovaara, P., Ehn, M., Kulmala, M., Tomlinson, J., Collins, D., Cubison, M., Dunlea, E., Huffman, J., Onasch, T., Alfarra, M., Williams, P., Bower, K., Kondo, Y., Schneider, J., Drewnick, F., Borrmann, S., Weimer, S., Demerjian, K., Salcedo, D., Cottrell, L., Griffin, R., Takami, A., Miyoshi, T., Hatakeyama, S., Shimono, A., Sun, J., Zhang, Y., Dzepina, K., Kimmel, J., Sueper, D., Jayne, J., Herndon, S., Trimborn, A., Williams, L., Wood, E., Middlebrook, A., Kolb, C., Baltensperger, U., and Worsnop, D.: Evolution of organic aerosols in the atmosphere, Science, 326, 1525–1529, doi:10.1126/science.1180353, 2009.

Kroll, J., Smith, J., Che, D., Kessler, S., Worsnop, D., and Wilson, K.: Measurement of fragmentation and functionalization pathways in the heterogeneous oxidation of oxidized organic aerosol, Phys. Chem. Chem. Phys., 11, 8005–8014, doi:10.1039/b905289e, 2009.

Kroll, J., Donahue, N., Jimenez, J., Kessler, S., Canagaratna, M., Wilson, K., Altieri, K., Mazzoleni, L., Wozniak, A., Bluhm, H., Mysak, E., Smith, J., Kolb, C., and Worsnop, D.: Carbon oxidation state as a metric for describing the chemistry of atmospheric organic aerosol, Nature Chem., 3, 133–139, doi:10.1038/nchem.948, 2011.

Lambe, A. T., Ahern, A. T., Williams, L. R., Slowik, J. G., Wong, J. P. S., Abbatt, J. P. D., Brune, W. H., Ng, N. L., Wright, J. P., Croasdale, D. R., Worsnop, D. R., Davidovits, P., and Onasch, T. B.: Characterization of aerosol photooxidation flow reactors: heterogeneous oxidation, secondary organic aerosol formation and cloud condensation nuclei activity measurements, Atmos. Meas. Tech., 4, 445–461, doi:10.5194/amt-4-445-2011, 2011.

Lanz, V., Alfarra, M., Baltensperger, U., Buchmann, B., Hueglin, C., Szidat, S., Wehrli, M., Wacker, L., Weimer, S., Caseiro, A., Puxbaum, H., and Prevot, A.: Source attribution of submicron organic aerosols during wintertime inversions by advanced factor analysis of aerosol mass spectra, Environ. Sci. Technol., 42, 214–220, doi:10.1021/es0707207, 2008.

Lanz, V. A., Prévôt, A. S. H., Alfarra, M. R., Weimer, S., Mohr, C., DeCarlo, P. F., Gianini, M. F. D., Hueglin, C., Schneider, J., Favez, O., D'Anna, B., George, C., and Baltensperger, U.: Char-

ACPD
15, 14403–14443, 2015

acterization of aerosol chemical composition with aerosol mass spectrometry in Central Europe: an overview, Atmos. Chem. Phys., 10, 10453–10471, doi:10.5194/acp-10-10453-2010, 2010.

Liu, P. S. K., Deng, R., Smith, K. A., Williams, L. R., Jayne, J. T., Canagaratna, M. R., Moore, K., Onasch, T. B., Worsnop, D. R., and Deshler, T.: Transmission efficiency of an aerodynamic focusing lens system: comparison of model calculations and laboratory measurements for the Aerodyne Aerosol Mass Spectrometer, Aerosol Sci. Tech., 41, 721–733, doi:10.1080/02786820701422278, 2007.

Marenco, F., Bonasoni, P., Calzolari, F., Ceriani, M., Chiari, M., Cristofanelli, P., D'Alessandro, A., Fermo, P., Lucarelli, F., Mazzei, F., Nava, S., Piazzalunga, A., Prati, P., Valli, G., and Vecchi, R.: Characterization of atmospheric aerosols at Monte Cimone, Italy, during summer 2004: source apportionment and transport mechanisms, J. Geophys. Res.-Atmos., 111, D24202, doi:10.1029/2006jd007145, 2006.

Marinoni, A., Cristofanelli, P., Calzolari, F., Roccato, F., Bonafe, U., and Bonasoni, P.: Continuous measurements of aerosol physical parameters at the Mt. Cimone GAW Station (2165 m a.s.l., Italy), Sci. Total Environ., 391, 241–251, doi:10.1016/j.scitotenv.2007.10.004, 2008.

Massoli, P., Lambe, A. T., Ahern, A. T., Williams, L. R., Ehn, M., Mikkila, J., Canagaratna, M. R., Brune, W. H., Onasch, T. B., Jayne, J. T., Petaja, T., Kulmala, M., Laaksonen, A., Kolb, C. E., Davidovits, P., and Worsnop, D. R.: Relationship between aerosol oxidation level and hygroscopic properties of laboratory generated secondary organic aerosol (SOA) particles, Geophys. Res. Lett., 37, L24801, doi:10.1029/2010gl045258, 2010.

Mensah, A. A., Holzinger, R., Otjes, R., Trimborn, A., Mentel, Th. F., ten Brink, H., Henzing, B., and Kiendler-Scharr, A.: Aerosol chemical composition at Cabauw, The Netherlands as observed in two intensive periods in May 2008 and March 2009, Atmos. Chem. Phys., 12, 4723–4742, doi:10.5194/acp-12-4723-2012, 2012.

Middlebrook, A. M., Bahreini, R., Jimenez, J. L., and Canagaratna, M. R.: Evaluation of composition-dependent collection efficiencies for the Aerodyne aerosol mass spectrometer using field data, Aerosol Sci. Tech., 46, 258–271, doi:10.1080/02786826.2011.620041, 2012.

Mohr, C., DeCarlo, P. F., Heringa, M. F., Chirico, R., Slowik, J. G., Richter, R., Reche, C., Alastuey, A., Querol, X., Seco, R., Peñuelas, J., Jiménez, J. L., Crippa, M., Zimmermann, R., Baltensperger, U., and Prévôt, A. S. H.: Identification and quantification of organic aerosol

ACPD
15, 14403–14443, 2015

from cooking and other sources in Barcelona using aerosol mass spectrometer data, Atmos. Chem. Phys., 12, 1649–1665, doi:10.5194/acp-12-1649-2012, 2012.
Morgan, W. T., Allan, J. D., Bower, K. N., Highwood, E. J., Liu, D., McMeeking, G. R., Northway, M. J., Williams, P. I., Krejci, R., and Coe, H.: Airborne measurements of the spatial distribution of aerosol chemical composition across Europe and evolution of the organic fraction, Atmos. Chem. Phys., 10, 4065–4083, doi:10.5194/acp-10-4065-2010, 2010.
Ng, N. L., Canagaratna, M. R., Zhang, Q., Jimenez, J. L., Tian, J., Ulbrich, I. M., Kroll, J. H., Docherty, K. S., Chhabra, P. S., Bahreini, R., Murphy, S. M., Seinfeld, J. H., Hildebrandt, L., Donahue, N. M., DeCarlo, P. F., Lanz, V. A., Prévôt, A. S. H., Dinar, E., Rudich, Y., and Worsnop, D. R.: Organic aerosol components observed in Northern Hemispheric datasets from Aerosol Mass Spectrometry, Atmos. Chem. Phys., 10, 4625–4641, doi:10.5194/acp-10-4625-2010, 2010.
Ng, N. L., Canagaratna, M. R., Jimenez, J. L., Chhabra, P. S., Seinfeld, J. H., and Worsnop, D. R.: Changes in organic aerosol composition with aging inferred from aerosol mass spectra, Atmos. Chem. Phys., 11, 6465–6474, doi:10.5194/acp-11-6465-2011, 2011.
Paatero, P. and Tapper, U.: Positive matrix factorization – a nonnegative factor model with optimal utilization of error-estimates of data values, Environmetrics, 5, 111–126, doi:10.1002/env.3170050203, 1994.
Pang, Y., Turpin, B. J., and Gundel, L. A.: On the importance of organic oxygen for understanding organic aerosol particles, Aerosol Sci. Tech., 40, 128–133, doi:10.1080/02786820500423790, 2006.
Petzold, A., Kramer, H., and Schonlinner, M.: Continuous measurement of atmospheric black carbon using a multi-angle absorption photometer, Environ. Sci. Pollut. R., 4, 78–82, 2002.
Prevot, A. S. H., Dommen, J., and Baumle, M.: Influence of road traffic on volatile organic compound concentrations in and above a deep Alpine valley, Atmos. Environ., 34, 4719–4726, doi:10.1016/s1352-2310(00)00254-5, 2000.
Putaud, J.-P., Van Dingenen, R., Dell'Acqua, A., Raes, F., Matta, E., Decesari, S., Facchini, M. C., and Fuzzi, S.: Size-segregated aerosol mass closure and chemical composition in Monte Cimone (I) during MINATROC, Atmos. Chem. Phys., 4, 889–902, doi:10.5194/acp-4-889-2004, 2004.
Saarikoski, S., Carbone, S., Decesari, S., Giulianelli, L., Angelini, F., Canagaratna, M., Ng, N. L., Trimborn, A., Facchini, M. C., Fuzzi, S., Hillamo, R., and Worsnop, D.: Chemical character-

ACPD
15, 14403–14443, 2015

ization of springtime submicrometer aerosol in Po Valley, Italy, Atmos. Chem. Phys., 12, 8401–8421, doi:10.5194/acp-12-8401-2012, 2012.
Schuepbach, E., Friedli, T. K., Zanis, P., Monks, P. S., and Penkett, S. A.: State space analysis of changing seasonal ozone cycles (1988–1997) at Jungfraujoch (3580 m a.s.l.) in Switzerland, J. Geophys. Res.-Atmos., 106, 20413–20427, doi:10.1029/2000jd900591, 2001.
Seinfeld, J. H. and Pankow, J. F.: Organic atmospheric particulate material, Annu. Rev. Phys. Chem., 54, 121–140, doi:10.1146/annurev.physchem.54.011002.103756, 2003.
Steinbacher, M., Zellweger, C., Schwarzenbach, B., Bugmann, S., Buchmann, B., Ordonez, C., Prevot, A. S. H., and Hueglin, C.: Nitrogen oxide measurements at rural sites in Switzerland: bias of conventional measurement techniques, J. Geophys. Res.-Atmos., 112, D11307, doi:10.1029/2006jd007971, 2007.
Sun, Y., Zhang, Q., Macdonald, A. M., Hayden, K., Li, S. M., Liggio, J., Liu, P. S. K., Anlauf, K. G., Leaitch, W. R., Steffen, A., Cubison, M., Worsnop, D. R., van Donkelaar, A., and Martin, R. V.: Size-resolved aerosol chemistry on Whistler Mountain, Canada with a high-resolution aerosol mass spectrometer during INTEX-B, Atmos. Chem. Phys., 9, 3095–3111, doi:10.5194/acp-9-3095-2009, 2009.
Sun, Y.-L., Zhang, Q., Schwab, J. J., Demerjian, K. L., Chen, W.-N., Bae, M.-S., Hung, H.-M., Hogrefe, O., Frank, B., Rattigan, O. V., and Lin, Y.-C.: Characterization of the sources and processes of organic and inorganic aerosols in New York city with a high-resolution time-of-flight aerosol mass apectrometer, Atmos. Chem. Phys., 11, 1581–1602, doi:10.5194/acp-11-1581-2011, 2011a.
Sun, Y. L., Zhang, Q., Schwab, J. J., Chen, W. N., Bae, M. S., Lin, Y. C., Hung, H. M., and Demerjian, K. L.: A case study of aerosol processing and evolution in summer in New York City, Atmos. Chem. Phys., 11, 12737–12750, doi:10.5194/acp-11-12737-2011, 2011b.
Takegawa, N., Miyakawa, T., Kawamura, K., and Kondo, Y.: Contribution of selected dicarboxylic and omega-oxocarboxylic acids in ambient aerosol to the m/z 44 signal of an aerodyne aerosol mass spectrometer, Aerosol Sci. Tech., 41, 418–437, doi:10.1080/02786820701203215, 2007.
Ulbrich, I. M., Canagaratna, M. R., Zhang, Q., Worsnop, D. R., and Jimenez, J. L.: Interpretation of organic components from Positive Matrix Factorization of aerosol mass spectrometric data, Atmos. Chem. Phys., 9, 2891–2918, doi:10.5194/acp-9-2891-2009, 2009.
Van Krevelen, D. W.: Graphical-statistical method for the study of structure and reaction processes of coal, Fuel, 24, 269–284, 1950.

ACPD
15, 14403–14443, 2015

Zhang, Q., Jimenez, J., Canagaratna, M., Allan, J., Coe, H., Ulbrich, I., Alfarra, M., Takami, A., Middlebrook, A., Sun, Y., Dzepina, K., Dunlea, E., Docherty, K., DeCarlo, P., Salcedo, D., Onasch, T., Jayne, J., Miyoshi, T., Shimono, A., Hatakeyama, S., Takegawa, N., Kondo, Y., Schneider, J., Drewnick, F., Borrmann, S., Weimer, S., Demerjian, K., Williams, P., Bower, K., Bahreini, R., Cottrell, L., Griffin, R., Rautiainen, J., Sun, J., Zhang, Y., and Worsnop, D.: Ubiquity and dominance of oxygenated species in organic aerosols in anthropogenically-influenced Northern Hemisphere midlatitudes, Geophys. Res. Lett., 34, L13801, doi:10.1029/2007gl029979, 2007.

Zhang, Q., Jimenez, J., Canagaratna, M., Ulbrich, I., Ng, N., Worsnop, D., and Sun, Y.: Understanding atmospheric organic aerosols via factor analysis of aerosol mass spectrometry: a review, Anal. Bioanal. Chem., 401, 3045–3067, doi:10.1007/s00216-011-5355-y, 2011.

ACPD
15, 14403–14443, 2015

Table 1. Summary of AMS measurements at mountain sites published in the literature.

Reference	Site/Season	Altitude (m a.s.l.)	Organics	Nitrate	Sulphate	Ammonium	Chloride	H : C	O : C	OM : OC
Hock et al. (2008)	Hohenpeissenberg/ spring	985	3.4 (50 %)	1.3 (19 %)	1.3 (19 %)	0.7 (11 %)	0.07 (1 %)	–	–	–
Sun et al. (2009)	Whistler Mountain/ spring	2182	1.05 ± 1.03 (55 %)	0.05 ± 0.10 (3 %)	0.58 ± 0.41 (30 %)	0.23 ± 0.16 (12 %)	–	1.66 ± 0.06	0.83 ± 0.17	2.28 ± 0.23
Lanz et al. (2010)	Jungfraujoch/ spring	3580	0.7 (43 %)	0.3 (18 %)	0.4 (26 %)	0.2 (13 %)	< 0.02 (< 1 %)	–	–	–
Freney et al. (2011)	puy-de-Dôme/ autumn	1465	2.52 (34 %)	1.14 (15 %)	2.4(32 %)	1.36 (18 %)	0.02 (0.3 %)	–	–	–
Freney et al. (2011)	puy-de-Dôme/ winter	1465	1.24 (23 %)	1.71 (32 %)	1.28 (24 %)	1.08 (20 %)	0.07 (1 %)	–	–	–
Freney et al. (2011)	puy-de-Dôme/ summer	1465	15.59 (57 %)	2.33 (9 %)	5.45 (20 %)	3.69 (14 %)	0.06 (0.2 %)	–	–	–

ACPD
15, 14403–14443, 2015

Table 2. Pearson correlation coefficients (R) between the time series of the three PMF factors and several gas-phase and particle tracers measured at Mt. Cimone. BC = black carbon, CO = carbon monoxide, T = air temperature P = atmospheric pressure, RH = relative humidity, WS = wind speed, UVB = UVB radiation flux, O_3 = ozone.

	BC	CO	T	P	RH	WS	UVB	O_3	NO_x	Nitrate	Sulphate	Ammonium
OOAa	0.54	0.71	0.48	0.42	0.22	−0.23	0.12	0.45	0.70	0.55	0.48	0.57
OOAb	0.35	0.27	0.36	0.25	−0.01	0.02	0.09	0.28	0.18	0.09	0.64	0.43
OOAc	0.41	0.24	0.16	0.26	−0.12	0.12	−0.10	0.58	0.02	0.12	0.49	0.38

ACPD
15, 14403–14443, 2015

Table 3. Pearson correlation coefficients (R) between the profiles of the three PMF factors and reference high resolution factor profiles found in the literature. OOA = oxygenated organic aerosol, HOA = hydrocarbon-like organic aerosol, BBOA = biomass burning organic aerosol, NOA = nitrogen containing organic aerosol, LVOOA = low volatility oxygenated organic aerosol, SVOOA = semi-volatile oxygenated organic aerosol.

	Saarikoski et al. (2012)						Mohr et al. (2012)				Crippa et al. (2013)		
	OOAa	OOAb	OOAc	HOA	BBOA	NOA	BBOA	HOA	LVOOA	SVOOA	SVOOA	LVOOA	HOA
OOAa	0.93	0.92	0.90	0.75	0.38	0.40	0.62	0.19	0.87	0.81	0.86	0.93	0.50
OOAb	0.94	0.92	0.90	0.70	0.30	0.34	0.61	0.17	0.91	0.81	0.81	0.93	0.45
OOAc	0.97	0.94	0.97	0.58	0.21	0.10	0.31	0.07	0.95	0.76	0.59	0.94	0.32

ACPD
15, 14403–14443, 2015

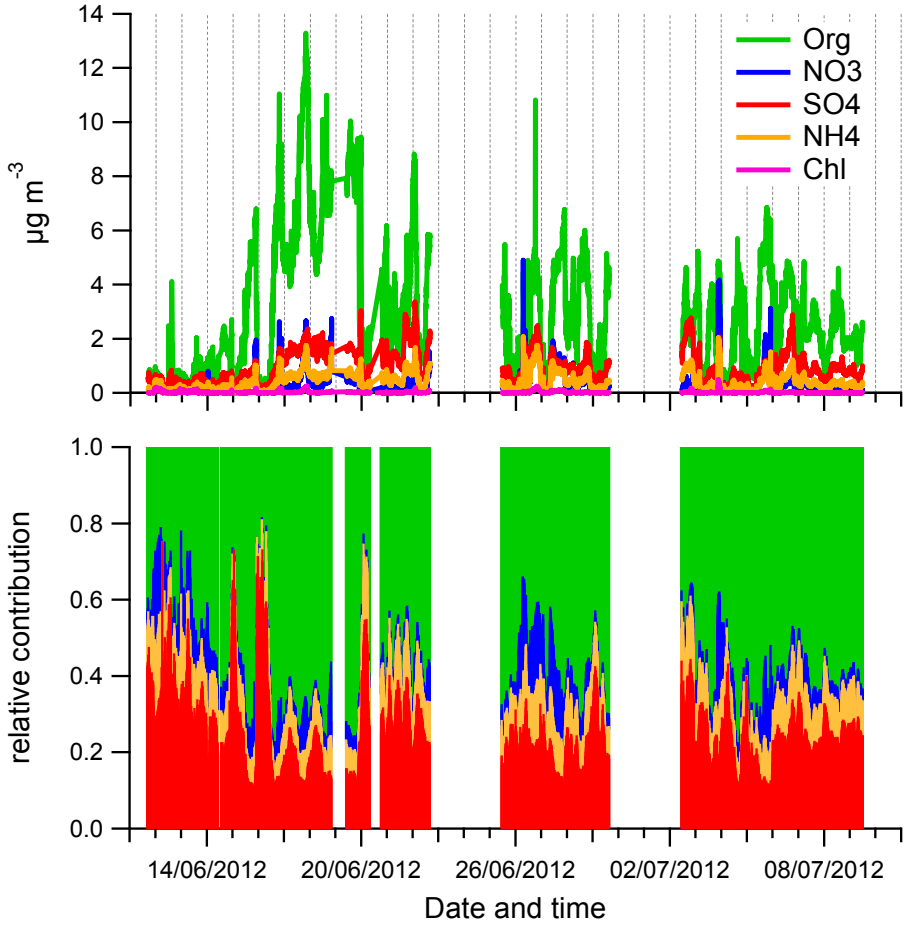

Figure 1. Time series and relative contribution of the main NR-PM_1 components.

ACPD
15, 14403–14443, 2015

Organic aerosol evolution and transport observed at Mt. Cimone

M. Rinaldi et al.

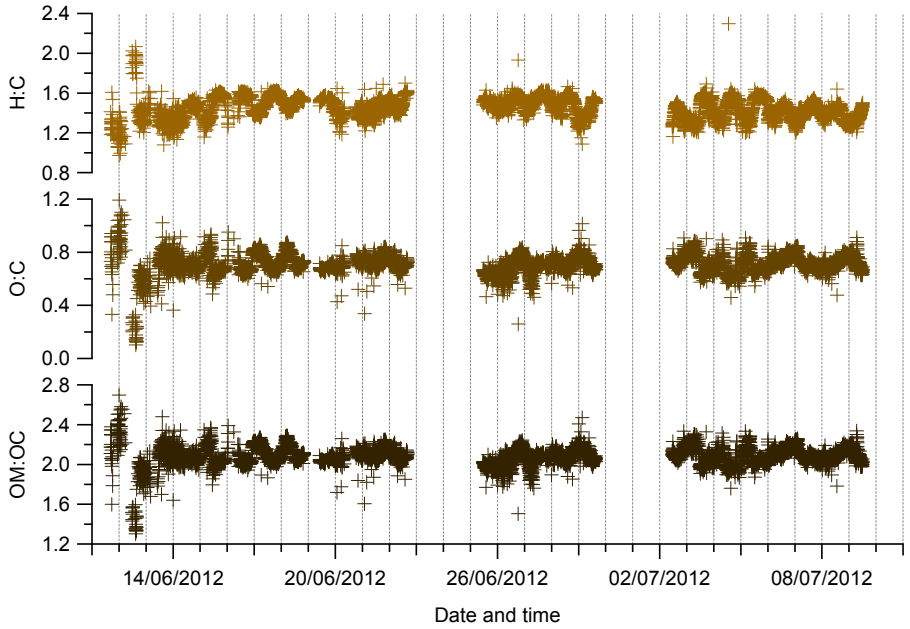

Figure 2. Time series of the H : C, O : C and OM : OC ratios.

ACPD
15, 14403–14443, 2015

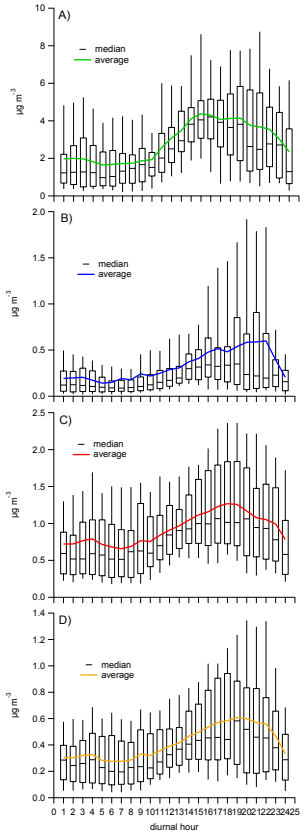

Figure 3. Daily trends of **(a)** organics, **(b)** nitrate, **(c)** sulphate and **(d)** ammonium. Boxes represent median, 25th and 75th percentile; whiskers indicates 10th and 90th percentile.

ACPD
15, 14403–14443, 2015

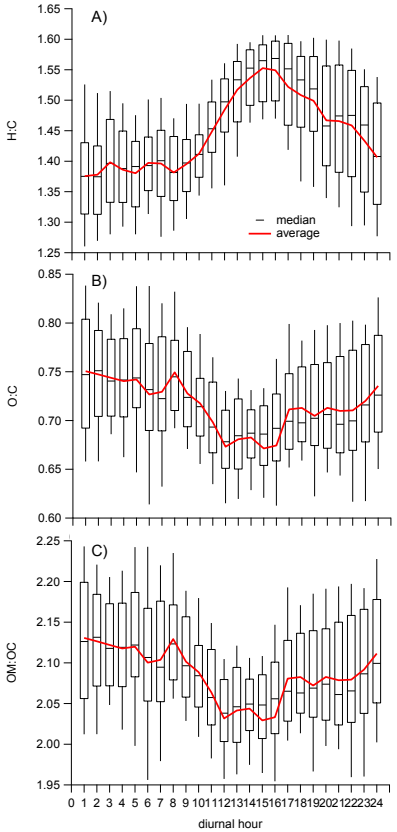

Figure 4. Daily trends of the **(a)** H : C, **(b)** O : C and **(c)** OM : OC ratios. Boxes represent median, 25th and 75th percentile; whiskers indicates 10th and 90th percentile.

ACPD
15, 14403–14443, 2015

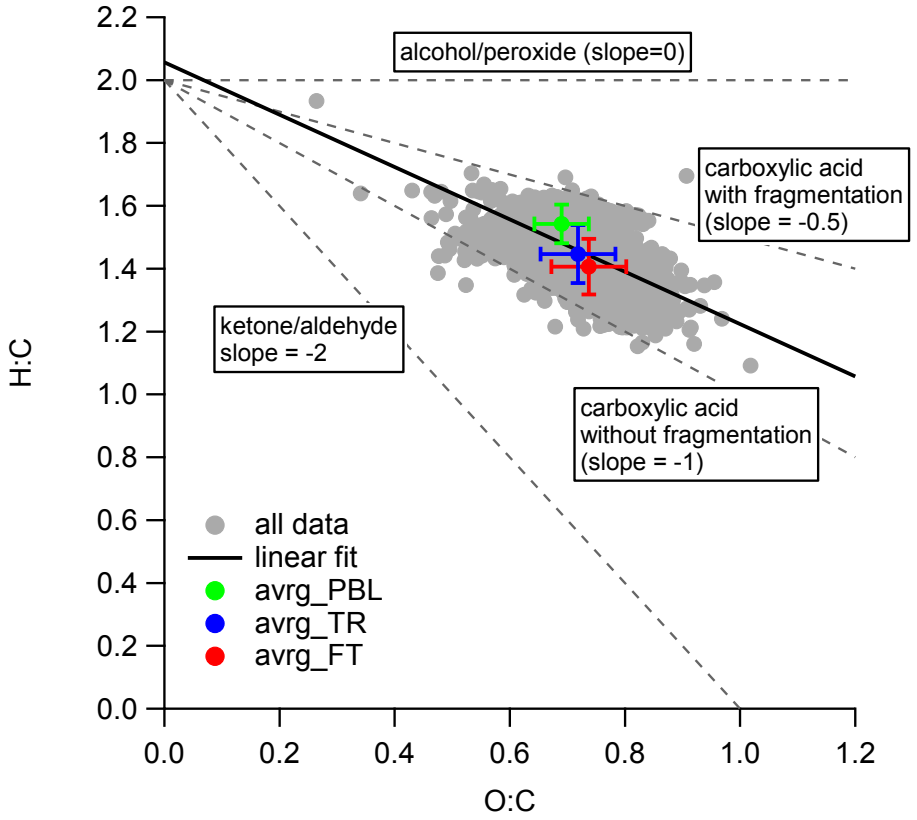

Figure 5. Van Krevelen diagram presenting the H : C and O : C ratios of all the data points collected during the campaign, superimposed to average values for PBL, TR and FT samples. Dashed lines describes oxidation reactions occurring through addition of carbonyl groups (slope = −2, Heald et al., 2010), carboxylic acid without fragmentation (slope = −1, Heald et al., 2010), carboxylic acid with fragmentation (slope = −0.5, Ng et al., 2011) and alcohol/peroxide (slope = 0, Heald et al., 2010).

ACPD
15, 14403–14443, 2015

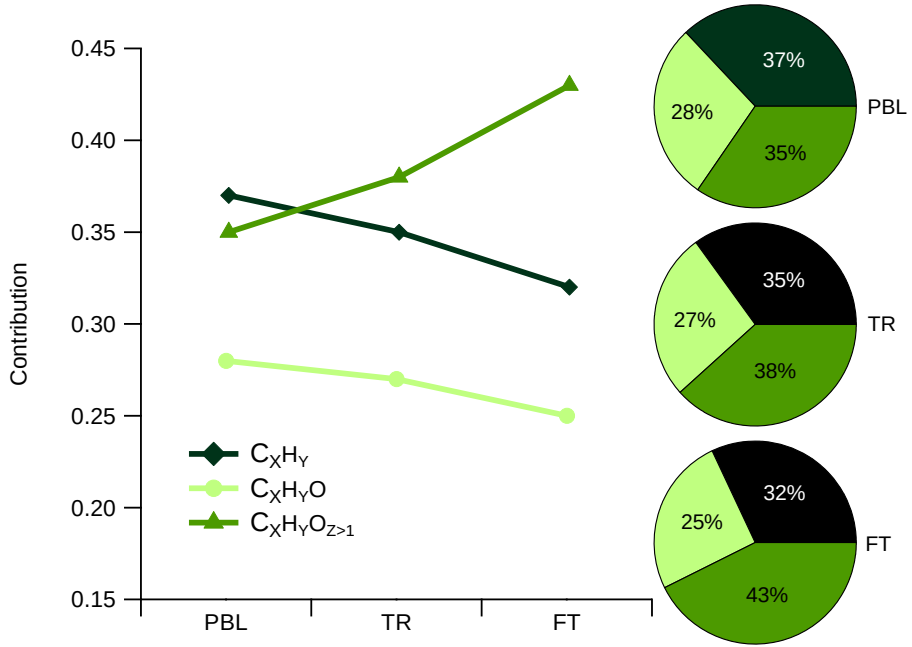

Figure 6. Contribution of organic fragments containing only carbon and hydrogen (C_xH_y), organic fragments containing carbon, hydrogen and one oxygen atom ($C_xH_yO_1$) and organic fragments containing carbon, hydrogen and more than one oxygen atom ($C_xH_yO_{z>1}$) in PBL, TR and FT samples.

ACPD
15, 14403–14443, 2015

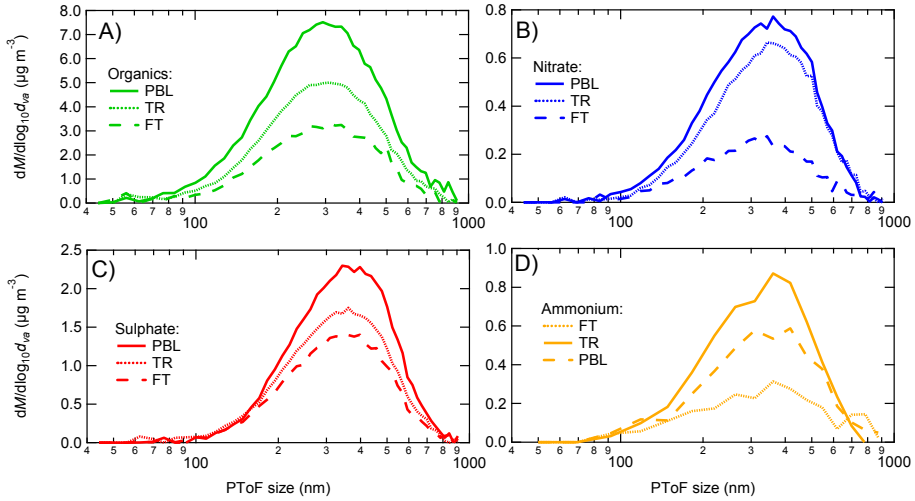

Figure 7. Size distribution of **(a)** organics, **(b)** nitrate, **(c)** sulphate and **(d)** ammonium in PBL, TR and FT samples.

ACPD
15, 14403–14443, 2015

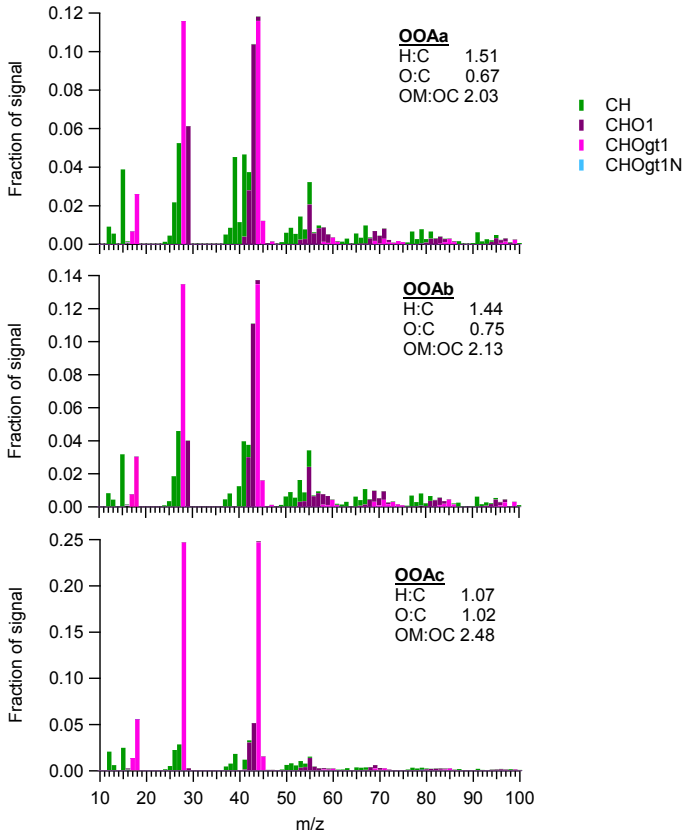

Figure 8. High resolution mass spectra of the three factors extracted by PMF. Insets in each plot reports the results of the elemental analysis.

ACPD
15, 14403–14443, 2015

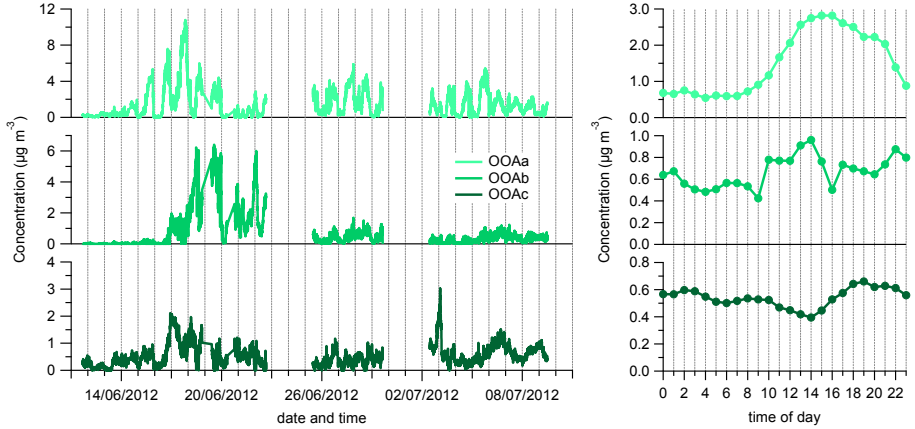

Figure 9. Time series and diurnal trend of the three factors extracted by PMF.

ACPD
15, 14403–14443, 2015

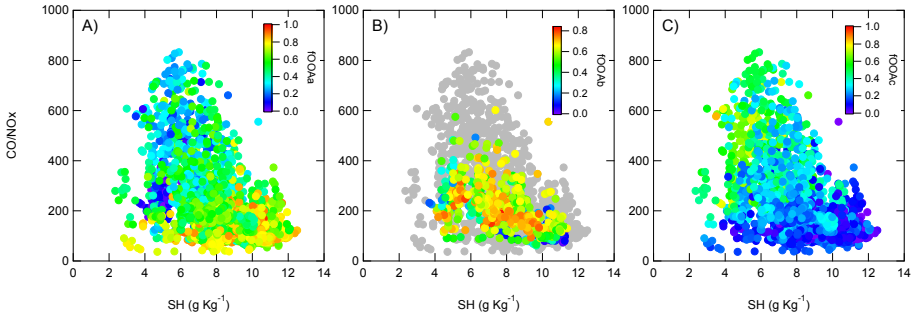

Figure 10. CO / NO_x ratio vs. SH, colour coded by the contribution of factors **(a)** OOAa, **(b)** OOAb and **(c)** OOAc. In **(b)** only the data points corresponding to OOAb maximum contribution period (17–23 June) have been coloured, to make the plot clearer.

ACPD
15, 14403–14443, 2015